Review

# Force probing cell shape changes to molecular resolution

Martin P. Stewart[1,2], Yusuke Toyoda[2], Anthony A. Hyman[2] and Daniel J. Muller[1]

[1] ETH Zurich, Biosystems Science and Engineering, CH-4058 Basel, Switzerland
[2] Max Planck Institute of Molecular Cell Biology and Genetics, D-01307 Dresden, Germany

**Atomic force microscopy (AFM) is a force sensing nanoscopic tool that can be used to undertake a multiscale approach to understand the mechanisms that underlie cell shape change, ranging from the cellular to molecular scale. In this review paper, we discuss the use of AFM to characterize the dramatic shape changes of mitotic cells. AFM-based mechanical assays can be applied to measure the considerable rounding force and hydrostatic pressure generated by mitotic cells. A complementary AFM technique, single-molecule force spectroscopy, is able to quantify the interactions and mechanisms that functionally regulate individual proteins. Future developments of these nanomechanical methods, together with advances in light microscopy imaging and cell biological and genetic tools, should provide further insight into the biochemical, cellular and mechanical processes that govern mitosis and other cell shape change phenomena.**

## Quantifying forces from cells to single molecules

The living cell is a highly specialized system that has evolved manifold ways to precisely control biochemical and biophysical interactions that regulate its molecular machinery. Biomolecular interactions generate tiny forces ranging from piconewtons ($10^{-12}$ N) to nanonewtons ($10^{-9}$ N) that persist over time spans from milliseconds to many minutes or more. On the cellular level these interactions can converge to drive considerable microscopic processes such as migration, motility, adhesion, cell shape change and division. But how cells establish and regulate these interactions to operate basic cellular processes remains, in many cases, mysterious.

In the past two decades, tremendous progress has been made in developing force spectroscopy methods to quantify chemical and physical interactions that contribute to cellular and biomolecular systems [1–5]. Most of these methods are based on atomic force microscopy (AFM), optical and magnetic tweezers, and microneedles [6–9]. These methods all use mechanical force probes such as cantilever styluses, beads, vesicles or microneedles to measure biomolecular interactions. The large breadth in force resolution of these probes (from $\sim 10^{-4}$ to $10^{3}$ nN) has enabled the measurement of forces as tiny as a few hydrogen bonds up to those required for separating two adhering cells. When applying forces to manipulate and quantify single molecules, these methods are commonly described as single-molecule force spectroscopy (SMFS).

Most SMFS applications characterize the interaction of a purified biomolecular system. Such *in vitro* experiments have an inherent flaw because they characterize biomolecules that are removed from the cellular context, which controls their assembly and functional state. Deciphering how cells control biomolecular interactions in the highly complex and dynamic environment of their interior requires transferring SMFS to the living cell. To approach *in vivo* experiments, SMFS can be applied from the outside of the cell to characterize interactions on or beneath the cell surface [10]. However, using SMFS to characterize cellular processes inside the living cell remains a challenge for the future [11]. Complementary to SMFS, single-cell force spectroscopy (SCFS) characterizes the interactions within an entire living cell [12]. These include, for example cell adhesion or mechanics [3,13–15]. Among the various SMFS and SCFS methods, the AFM-based approach provides the widest force resolution ranging from ≈10 pN to several hundreds of nN, which is in principle sufficiently sensitive to detect the binding of a single ligand to a single receptor and sufficiently strong to quantify the adhesion and mechanical properties of a living cell [7,10,12].

Invented in the early 1990 s, AFM-based SMFS is routinely applied to quantify the inter- and intramolecular interactions of single proteins, nucleic acids, oligosaccharides, lipids and membranes [1,2,5,7,10]. Such interactions can be of chemical or physical origin and include hydrophobic, hydrophilic, electrostatic, van der Waals, ionic or steric forces [16]. Biological systems and processes characterized by SMFS include ligand–receptor binding [1,3], protein (un-)folding [4,5], motor proteins at work [7], functional states of proteins [8,17], protein–protein and protein–nucleic acid interactions, mechanical elasticity of polymers, molecular and cellular adhesion, and biochemical recognition [2,3,10,12]. In principle, SMFS attaches one end of a molecule to the tip of the AFM cantilever and the other end of the molecule to a support. Separating the AFM tip from the support elongates the biomolecule until it adopts a stretched conformation. Upon further separation a mechanical stress is applied and the elastic molecule becomes elongated. If the molecule is a protein it can unfold. If the tip is functionalized by a ligand and the support by a receptor, approaching both allows ligand and receptor to bind, whereas separation ruptures the ligand–receptor bond [3]. The deflection of the AFM cantilever measures the force of these processes and thus quantifies their interactions.

In this review, we will emphasize how AFM-based SMFS and mechanical assays can be exploited in combination with

*Corresponding author:* Muller, D.J. (daniel.mueller@bsse.ethz.ch).

 0968-0004/$ – see front matter © 2011 Elsevier Ltd. All rights reserved. doi:10.1016/j.tibs.2011.05.001 

modern cell biological tools to characterize basic cell biological phenomena, such as mitotic cell rounding, to molecular resolution. The shape of most adherent cultured animal cells is flat and elongated, but it changes dramatically as cells enter mitosis [18], reduce their adherence to the substrate and round up, leaving retraction fibers attached to the substrate [19]. Cells remain round until cytokinesis, when cleavage furrow ingression divides the cell in two. Shape changes involved in cytokinesis, in particular, depend on the actomyosin cortex, a dynamic association of actin filaments and myosin motors [20,21], which constitutes a major component of the cellular cytoskeleton. Our understanding of the mechanics of cytokinesis has been advanced by studies using both light microscopy [22–25] and mechanical techniques such as micropipette aspiration to study surface forces [26], micromanipulation experiments [27], and spatially resolved AFM stiffness measurements of furrow dynamics [28]. Whereas cytokinesis has been somewhat widely studied, the mechanics of mitotic cell rounding, which is thought to be important for organization within the mitotic cell and to facilitate the geometric requirements of division, has received less attention to date [29–31]. The actomyosin cytoskeleton relocates to the cell periphery in the form of a homogeneous cortical layer and brings about retraction of the cell margin and stiffening of the cell surface during mitotic cell rounding [19,32]. This process depends on the upstream regulator RhoA [32] and membrane–cortex linkers, such as the ERM protein moesin [33,34]. However, the question of how forces are generated to drive the drastic morphological change of a mitotic cell remains an open question. Here, we outline the use of AFM to quantify the forces driving mitotic cell rounding, determine the cellular mechanisms which underpin the process and characterize the interactions regulating one such key protein, the $Na^+/H^+$-antiporter, to molecular resolution. Importantly, the unique application of AFM-based cell mechanics and SMFS in combination with modern cell biological tools is not restricted to the characterization of mitotic processes and can in principle be applied to unravel numerous other basic cell mechanical processes.

## Force probing mitotic cells

Mitotic cell rounding has been observed within the tissue of living organisms, in which mitotic cells are confined by their surrounding cells and extracellular matrix (Figure 1a) [29,35,36]. To simulate an impediment, such as would be present when a cell is surrounded by tissue, and to measure the forces driving cell rounding, we recently developed a method that employed a stationary tipless AFM cantilever to confine mitotic cells (Figure 1b) [37]. As the cells entered mitosis, they abandoned their flat morphology and attempted to round up against the cantilever; however, they were constrained to a near cylindrical shape (Figures 1b and 2a). The resultant upward force was recorded and divided by the contact area of the cell, as determined by light microscopy, to estimate a normalized 'rounding pressure' (Figure 2b). To demarcate the increase of force and rounding pressure in mitosis from the more general effect of a flat cell de-adhering from a substrate, individual G2/Prophase cells that had been prerounded with trypsin were followed through mitosis (Figure 2c). Despite cell size remaining relatively constant, the rounding pressure increased by more than 3-fold after cells entered mitosis (Figure 2d).

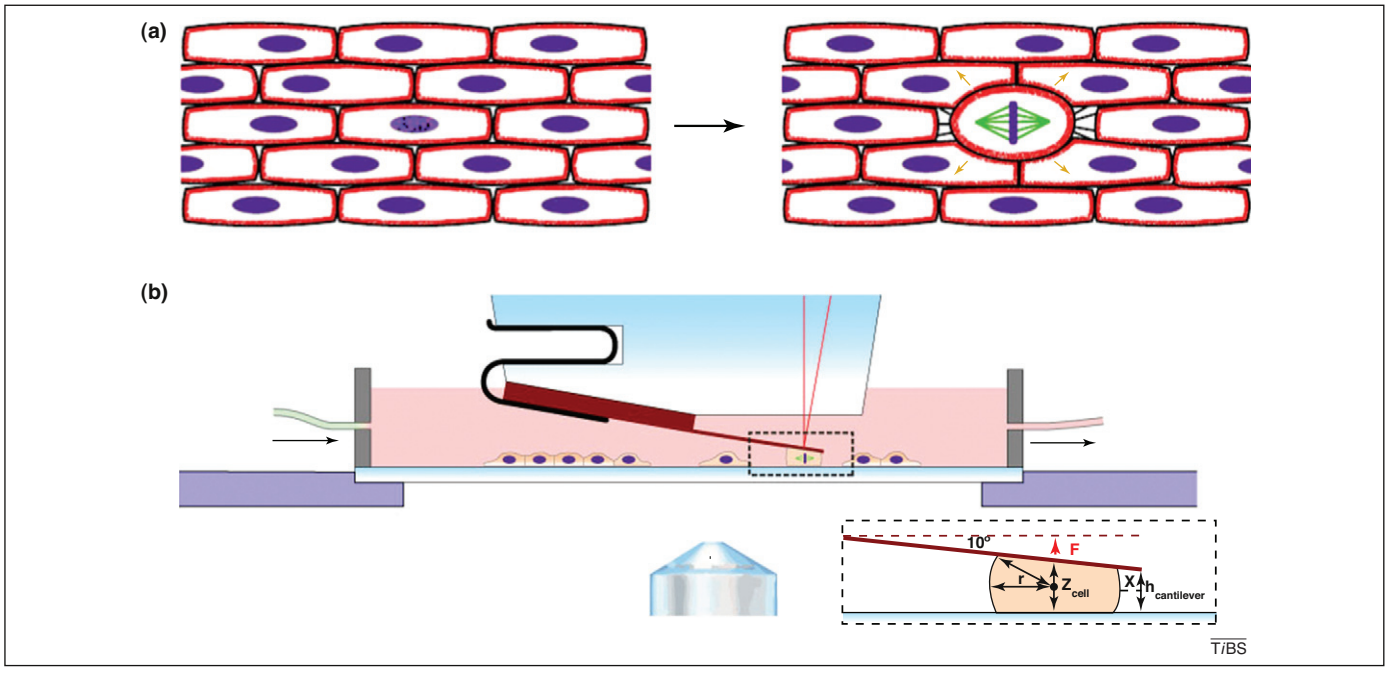


**Figure 1**. AFM-based assay to quantify the force and pressure driving mitotic cell rounding. **(a)** A schematic of mitotic cell rounding in a densely packed tissue environment. To round-up for mitosis, cells must create force (yellow arrows) to deform the surrounding cells. **(b)** An assay developed to measure such forces. A combined AFM and light microscope setup can measure the force, *F*, of, and observe, mitotic cell rounding at conditions mimicking the constraints of a tissue. A cell is confined under the cantilever and resistance forces are measured. Using light microscopy to measure the cross-sectional area of the cell, the rounding pressure, *RP*, can be derived by $RP = F/A$. Knowing the height of the middle of the cell, $z_{cell}$, and estimating the shape of the cell, it is also possible to calculate the cell volume, $V \approx \pi \times z_{cell}(r^2 - z_{cell}^2/12)$. Inhibitors and compounds of interest can be introduced to the cell by pumping them through the cell medium chamber via inlet and outlet ducts. In this way, it is possible to perturb pressure and volume homeostasis of a single live cell during a real-time measurement.

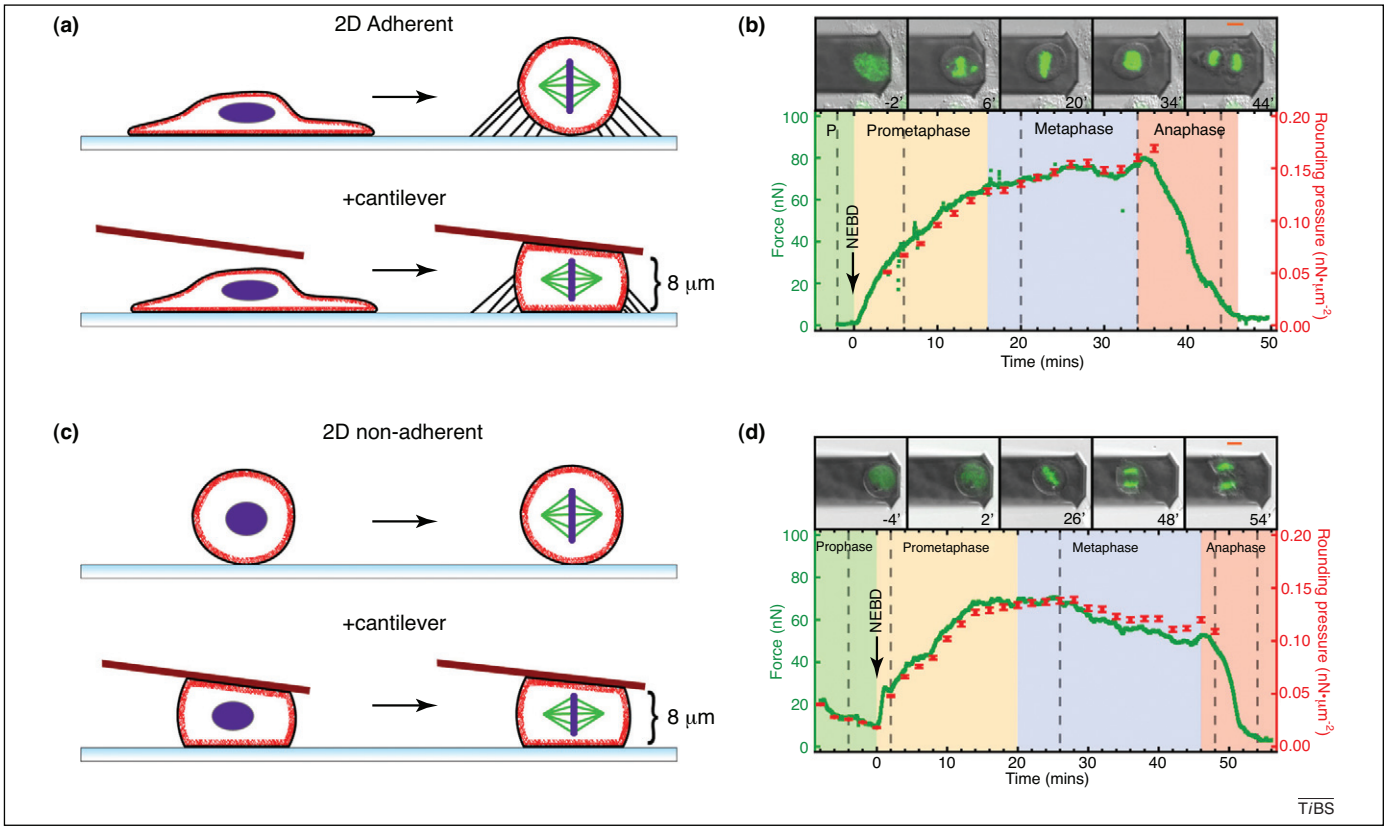


**Figure 2**. Characterizing the force and pressure that drives cell shape change. **(a)** A schematic depicting the transition from a flat adherent interphase cell into a round mitotic cell with retraction fibers. Confining the cellular shape change with a cantilever enables the measurement of forces that drive shape change. **(b)** Data from a single HeLa cell subjected to the scenario illustrated in **(a)**. A tipless cantilever (spring constant ≈ 0.3 N/m) is placed above a prophase cell at 8 μm above the substrate. The measured upward force (green) and calculated rounding pressure (red) are depicted; note that these measurements could be derived only while the cell was near cylindrical **(b)**. Displayed above the AFM data are overlaid differential interference contrast (DIC) and histone H2B–GFP images of a mitotic HeLa cell at the times indicated by the gray dashed lines. To correlate the mitotic state to the rounding force and pressure generated, the HeLa cells stably expressed histone H2B–GFP as chromatin marker. Time zero denotes nuclear envelope breakdown (NEBD). Mitotic phases are colored as follows: prophase (P, green), prometaphase (orange), metaphase (blue) and anaphase (red). Scale bar, 10 μm. **(c)** A schematic depicting a nonadherent (trypsinized) HeLa cell on a surface in transition from interphase to mitosis. **(d)** Data from a single mitotic cell subjected to the scenario in **(c)** but with the same assay presented in **(b)**. Even without significant shape change, the rounding force and pressure increase ≈3-fold in the transition from G2/prophase to metaphase. Panels **(b)** and **(d)** are reprinted with permission from Macmillan Publishers Ltd: Nature 469, 226–230, copyright (2011).

To determine which cellular mechanisms could generate the increased rounding pressure exhibited by mitotic cells, specific biochemical perturbations were conducted with mechanical measurements [37]. Inhibitors targeting the actomyosin cortex such as the F-actin barbed end capper cytochalasin D, the actin monomer sequester latrunculin A, the myosin II inhibitor blebbistatin and the ROCK inhibitor Y27632, all caused a decrease in cellular rounding pressure. By contrast, agents which dissolve the microtubule cytoskeleton prompted a minor increase in rounding pressure, probably because Rho GEF-H1 was no longer inhibited [38]. In addition to these observed differences in mechanical properties, discrete volume changes often accompanied fast-acting perturbations. For example, latrunculin A caused an increase in volume and a decrease in pressure (Figure 3a,b). Moreover, the permeabilization of the plasma membrane using pore-forming toxins, such as *Staphylococcus aureus* α-toxin or the exotoxin α-hemolysin, led to cell shrinkage and a decline in pressure (Figure 3a,b). α-Toxin-induced shrinkage was partly dependent upon the actomyosin cytoskeleton; it could be reduced if the cells were pretreated with latrunculin A. Accordingly, hypo- and hypertonic shocks changed the volume and pressure of mitotic cells in the expected directions (Figure 3a,b). Overall, it became clear that the mitotic cell establishes an osmotic gradient to generate pressure that facilitates rounding. Indeed, the ability of the mitotic cell to maintain osmotic pressure was substantially compromised (–53±10%) with exposure to 5-(*N*-ethyl-*N*-isopropyl)amiloride (EIPA), an amiloride analog that inhibits the $Na^+/H^+$-antiporter, NHE1 (also called SLC9A1) (Figure 3a,b).

Taken together, these results showed that the actomyosin cortex contracts against an outward-directed osmotic pressure. From a biophysical point of view, the intracellular osmotic pressure is a scalar and cannot define cell shape. Thus, actomyosin cortex contraction directs the pressure into a defined cell shape. Together, actomyosin contraction and osmotic pressure establish a balanced, and most probably a highly regulated, system to control the dramatic cell shape changes that occur during mitosis [37]. This model has general implications for cell and tissue mechanics beyond just mitotic cell rounding: by locally modulating actomyosin–cortex-dependent surface tension and globally regulating osmotic pressure, cells can control their volume, shape, motility and mechanical properties. These concepts are in agreement with current knowledge on the physics of cell shape change [39], specifically in relation to development [40,41] and motility [42–44].

The above example highlights the fact that AFM-based force spectroscopy in combination with perturbation

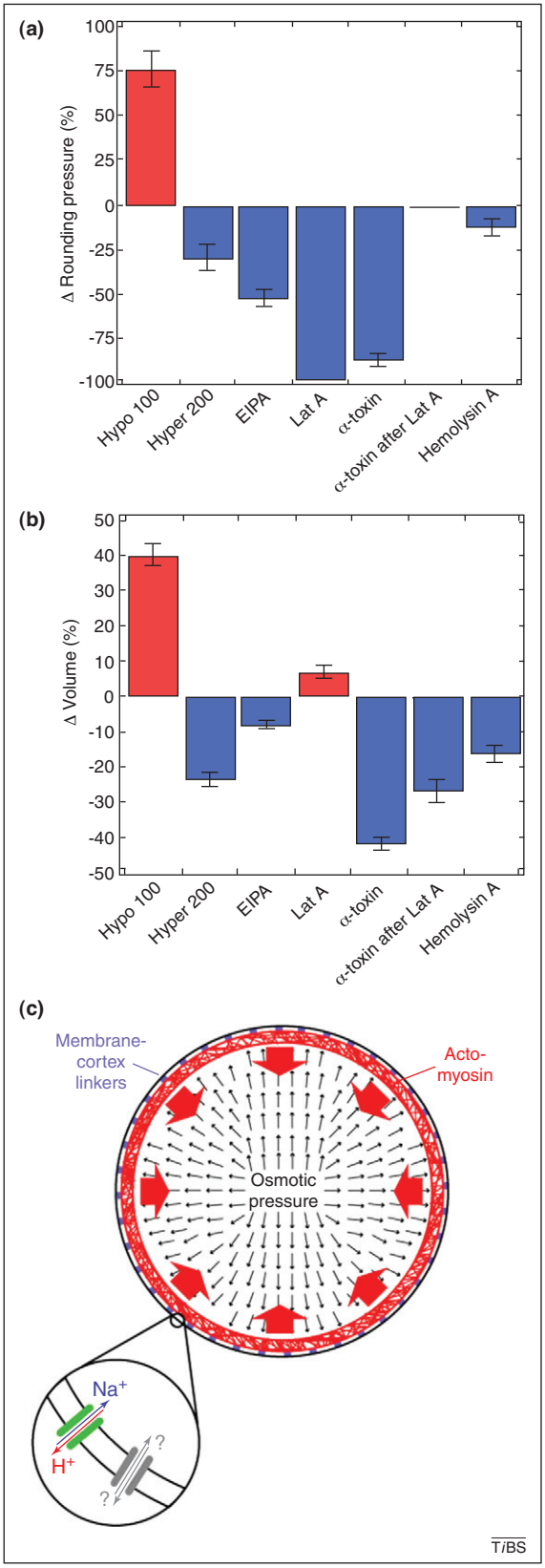


**Figure 3**. Actomyosin contraction and hydrostatic pressure govern the mechanics of mitotic cell rounding. **(a)** Relative changes in rounding pressure upon exposure of metaphase cells to indicated perturbants in an 8 μm constant height assay (Figure 2a,b, metaphase). Perturbations are Hypo 100 (–Δ100 mOsm/kg, hypotonic shock), Hyper 200 (+Δ200 mOsm/kg, hypertonic shock), EIPA [50 μM 5-(*N*-ethyl-*N*-isopropyl)amiloride], Lat A (1 μM Latrunculin A), α-toxin (60 μg/ml *Staphylococcus aureus* α-toxin), α-toxin after Lat A (1 μM Latrunculin A followed by 60 μg/ml *S. aureus* α-toxin after ~5 min) and hemolysin A (2 μg/ml). Changes shown for hypo- and hypertonic perturbations are the maximums exhibited before the cell responds with regulatory volume decrease (RVD) and regulatory volume increase (RVI), respectively. **(b)** Relative changes in volume upon exposure of metaphase cells in an 8 μm constant height assay (Figure 2b, metaphase) to the same perturbants as listed in **(a)**. **(c)** Uniform actomyosin contractile tension (red) is balanced by an outward-directed, intracellular osmotic pressure (black). Membrane–cortex linkers (purple) couple these two elements. The higher the tension and pressure, the greater the cortex rigidity. Imbalances between tension and osmotic pressure cause changes in cell volume and rounding force. The $Na^+$/$H^+$-antiporter (green) and probably other as yet uncharacterized osmolyte transporters (gray) govern the osmotic gradient and hence the hydrostatic pressure within cells during mitotic cell rounding.

experiments can be used to unravel basic mechanisms of cell shape change in mitosis. In this example, a protein was targeted that significantly contributes (up to 60%) to the osmotic gradient and pressure and thus rounding of the mitotic cell. In the following section, we describe how SMFS can be used to reveal insight into interaction mechanisms modulating the functional state of such a target.

## Force probing target proteins

When applied to water-soluble proteins or nucleic acids SMFS is limited in its ability to localize interactions on or in proteins or nucleic acids [1,5,7]. This is because a reference point is missing to structurally localize the force peak that characterizes an interaction. Such reference points can be introduced by mechanical triangulation, which engineers cysteine residues to control linkages of the protein topology [45]. However, this situation changes when applying SMFS to membrane proteins (Figure 4). Upon applying a mechanical pulling force to its terminal end, a membrane protein starts unfolding stepwise; beginning from the terminal end, one structural segment unfolds after the other until the entire membrane protein has been unfolded and extracted from the membrane [4]. Because the membrane holds back the unfolding intermediate of the membrane protein, it serves as a reference point. The separation between the pulling AFM tip and the membrane refers to the length of the unfolded and stretched polypeptide. Subtracting this length from the pulled terminal end allows to structurally locate the interaction and to quantify its strength by measuring its force. Intra- and intermolecular interactions structurally stabilize and determine the functional state of the protein. Thus, using SMFS to quantify the interactions of a membrane protein being set into different functional states allows localizing and learning which interactions stabilize their structure and which interactions modulate their functional state [17,46–48]. Similarly, SMFS can be used to quantify the interactions established upon binding of a molecular compound (e.g. ligand, substrate, drug), assembly with other proteins, lipids or biomolecules [4,48–50].

AFM-based experiments probing the mechanics of cell shape change in mitotic HeLa cells have identified the $Na^+$/$H^+$-antiporter NHE1 as a key membrane protein contributing to elevated osmotic pressure. This is perhaps not surprising considering existing data showing that the $Na^+$/$H^+$-antiporter (NHE1) is activated upon entry to mitosis [51] and induces the cytosolic pH increase characteristic of mitosis [52]. Moreover, $Na^+$/$H^+$ exchange plays a major role in regulatory volume increase after hypertonic shrinkage of cells [53]. Exchanging $H^+$ for $Na^+$ increases the intracellular osmolarity because pH is strongly buffered in the cytoplasm,

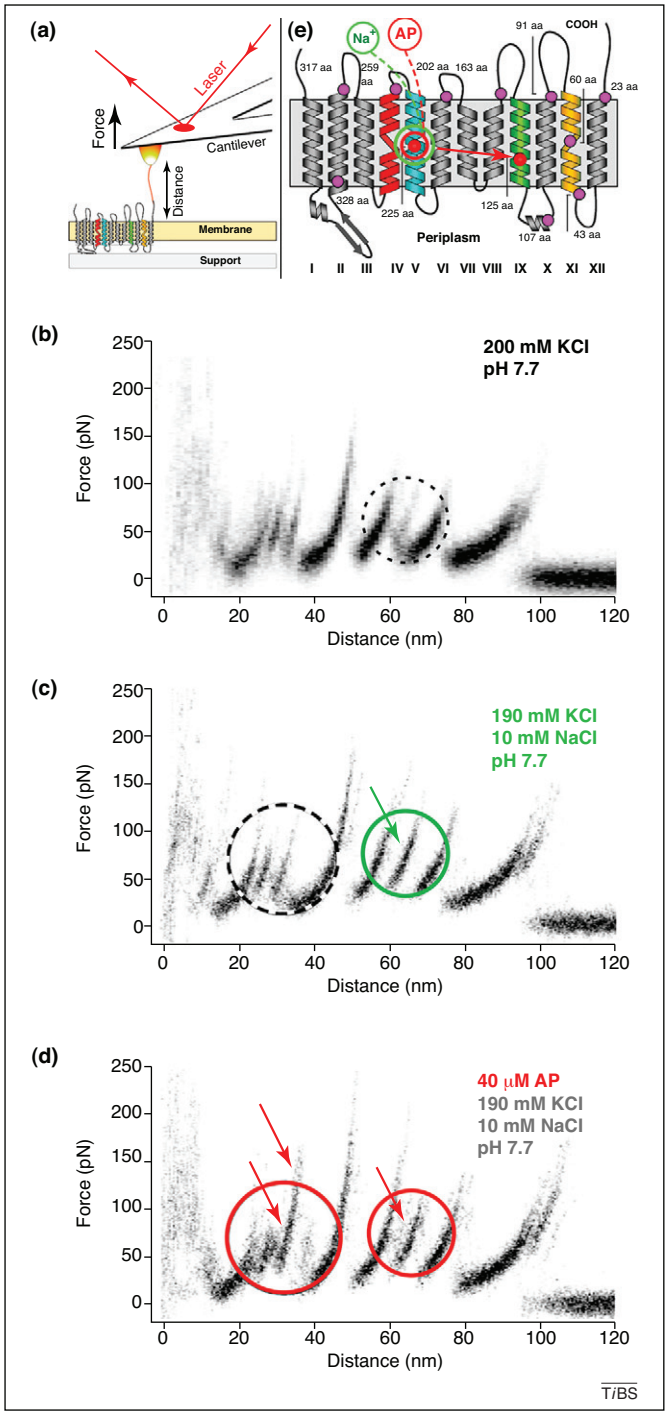


**Figure 4**. Applying SMFS to localize and quantify inter- and intramolecular interactions of a $Na^+/H^+$-antiporter. **(a)** The nanoscopic tip of the AFM cantilever is nonspecifically attached to the C terminal end of the antiporter. Withdrawal of the AFM tip stretches the C terminal end and deflects the cantilever. This deflection measures the force. At sufficiently high forces the antiporter starts a stepwise unfolding process. During the entire course of mechanical unfolding a force–distance (F–D) curve is recorded **(b–d)**. Force peaks of the F–D curve record the interaction strengths established by the antiporter, whereas the peak positions are used to structurally localize the interactions **(e)**. The amino acid (aa) regions establishing the interactions are located (purple spheres) taking the distance measuring the length of the unfolded polypeptide. In **(b)** the antiporter was unfolded in the absence of the ligand $Na^+$. Compared to the unfolding in the presence of the ligand **(c)**, the ligand has established an additional interaction highlighted by the green circle and arrow. This interaction locates to the ligand-binding pocket of the antiporter **(e)**, which is encircled at the center of the blue transmembrane α-helix V. The inhibitor 2-aminoperimidine (AP) **(d)** establishes the same interaction at the ligand-binding pocket as observed for $Na^+$. This interaction is highlighted by the single red arrow and the smaller red circle. However, in addition, the inhibitor significantly enhances an interaction denoted by the double red arrows and large red circle **(d)**. This additional interaction is located (red sphere) at the green transmembrane α-helix IX, where flexibility is functionally required. This interaction further stabilizes and restricts the conformational flexibility of α-helix IX **(e)**.

thus causing $Na^+$ to have a greater relative effect on osmolarity in comparison to $H^+$ [54,55]. Therefore, an increase in intracellular osmotic pressure triggered by $Na^+/H^+$-antiporter activity can be deployed both to drive volume recovery of hypertonically shrunken cells and shape changes such as mitotic cell rounding. In the following example, we will highlight how SMFS can be applied to reveal insight into interaction mechanisms regulating a $Na^+/H^+$-antiporter. Thus far, SMFS has to be conducted on membrane proteins that occur in densely packed assemblies of isolated membranes. Because there are no SMFS experiments available on human NHE1, we discuss discoveries made on the bacterial $Na^+/H^+$-antiporter NhaA from *Escherichia coli*. Although these findings cannot be directly translated to a mammalian context, it exemplifies the ability of an AFM-based platform to tackle such challenges.

Similar to NHE1, the $Na^+/H^+$-antiporter NhaA is involved in osmoregulation and pH homeostasis [56]. Moreover, NhaA is the only $Na^+/H^+$-antiporter whereby its structure has been solved by X-ray crystallography [57]. To characterize NhaA by SMFS, the antiporter was purified and reconstituted into *E. coli* lipids. Then, the NhaA-containing membranes were adsorbed to a support and imaged in buffer solution using high-resolution AFM [17,58]. After localizing individual membrane proteins, the AFM tip was gently pushed to a single antiporter to facilitate attachment of its C-terminal end. Upon withdrawing the AFM tip the C-terminal end was stretched and a mechanical pulling force applied (Figure 4a). At sufficiently high pulling forces (≈100–200 pN) the interaction stabilizing the first structural segment of NhaA ruptured and the structural segment unfolded. The unfolded polypeptide was extracted from the membrane and stretched until the interaction stabilizing the forthcoming structural segment was detected. All interactions were detected when unfolding the entire $Na^+/H^+$-antiporter during complete withdrawal of the AFM tip.

As a first step, SMFS was used to quantify the interactions of the NhaA antiporter in the absence of its ligand ($Na^+$) (Figure 4b) [17]. A force–distance (F–D) curve records the force over the pulling distance of the AFM tip (Figure 4b). The force peaks of the F–D curve quantify the interactions of NhaA that are mapped onto the tertiary structure of the antiporter (Figure 4e). Then, the $Na^+/H^+$-antiporter was functionally activated and exposed to the ligand. The F–D curves recorded of the active antiporter (Figure 4c) show one major difference to that of unliganded NhaA (Figure 4b) at a pulling distance of ≈65 nm. This pulling distance identifies an additional interaction at the center of transmembrane α-helix V, hosting aspartic residues 163 and 164, which are involved in the ligand-binding site. This interaction disappeared after the ligand was removed from the buffer solution [17]. Furthermore, the ligand was not able to establish this interaction with functionally inactive antiporters. Thus, this interaction is specific to ligand-binding and functional activation of NhaA.

Next, the interactions established upon binding of the inhibitor 2-aminoperimidine to NhaA were investigated [46]. F–D curves recorded in the presence of 2-aminoperimidine were different from those recorded of the inactive and from those recorded of the active $Na^+/H^+$-antiporter (Figure 4b–d). Similar to the ligand, the inhibitor established interactions at the ligand-binding pocket. These interactions were independent of the presence of the ligand [46]. However, the inhibitor established additional interactions that increased the stability of the transmembrane α-helix IX by ≈50%. The X-ray structure of NhaA suggests that α-helix IX fulfills certain roles [57]. First, α-helix IX is likely to be the structural element transmitting the pH signal required to activate NhaA. Second, the distortion of α-helix IX allows a high structural flexibility for a long-range conformational change. Third, α-helix IX at the membrane center is in direct contact with transmembrane α-helices IV and XI forming essential parts of the $Na^+/H^+$-exchange machinery. Thus, SMFS provided insight into the mechanism by which 2-aminoperimidine deactivates NhaA. First, the inhibitor binds and blocks the ligand-binding pocket. Second, it increases the interactions that stabilize α-helix IX (its flexibility is essential for proper functioning of the antiporter). The significantly strengthened interaction established at α-helix IX indicates that its flexibility has been reduced. Indeed, dynamic SMFS was able to show that the energy valley stabilizing this α-helix reduces in width upon inhibitor-binding [47]. This reduction of the energy valley reduces the number of conformational substates and, thus, the flexibility of α-helix IX.

## Concluding remarks

In this review, we described how AFM-based spectroscopy was used to unravel the basic mechanisms that stimulate the rounding of mitotic cells. This approach can be used to target proteins of interest that contribute to the generation of the osmotic pressure that drives this shape change. The identified target can then be probed with force spectroscopy to examine, identify and quantify the interactions and interaction mechanisms by which the target is functionally modulated. Such an approach provides insight, for example, into how these targets are functionally modulated *in vivo* and provides novel ways in which to manipulate their functional state.

AFM-based approaches open an exciting and promising avenue towards characterizing mechanisms driving cell shape to molecular resolution. One limitation of AFM-based force spectroscopy (and other existing force spectroscopy approaches) is the current difficulty in directly measuring interactions of biomolecules inside the living cell without perturbing the cellular integrity [11]. Thus, bringing SMFS into the living cell will be a major challenge. With further development, these approaches will, in the future, also become even more accurate and lead to even more sophisticated ways to illuminate basic cell biological mechanisms [6,8]. For example, combining AFM-based imaging and force spectroscopy allows the detection of the dynamic distribution and reassembly of membrane receptors of living cells [2,10]. Combined with fluorescence microscopy this approach allows optical imaging of membrane receptors and the use of AFM to identify receptors being functionally active [59]. For cell mechanics, the versatility of AFM can be further exploited to probe the mechanical properties of cells locally with a pyramidal or spherical tip [28,60], or globally by using flat tipless cantilevers in parallel plate configuration [37,61]. This range of methods has provided insight into how the cell responds to the activation of membrane receptors [59,62,63] and have shown how the nano- and micromechanical properties of the cell surface change with the functional state of tissue culture cells [28,64–66] and those extracted from living tissue [60,67,68]. Moreover, AFM has been used to characterize the lamellipodial protrusive forces generated in a migrating cell [69], forces generated by actin networks *in vitro* [70], forces modulated by the actomyosin cortex *in vivo* [15,60,71] and the contraction dynamics of single platelet cells [61]. After applying such setups as assays to screen for the target proteins that are responsible for the force generating mechanisms, it is then possible to apply SMFS to discover how these proteins are regulated. Thus, in the future one can envision using AFM to harvest quantitative information pertaining to fundamental cell biological phenomenon and to provide understanding of the mechanisms that regulate key molecular players in such cellular processes.

The potential of AFM can be further leveraged when combined with modern optical microscopy. This combination will make it possible to optically image cytoskeletal reassembly or to follow cytoplasmic processes and trafficking while mechanically probing the cell. In combination with modern cell biological and genetic tools, it will be then possible to specifically perturb or highlight cell biological processes contributing to cell shape changes, cell mechanics and cell adhesion. We envision that in the forthcoming decade the unique possibilities of AFM to directly quantify and manipulate biological systems will enable the characterization of physical properties from single molecules and macromolecular complexes all the way up to cells, tissues and organs. Such approaches should yield powerful new insights and discoveries in basic biology and physiology.

## Acknowledgments

Financial support from the Swiss National Competence Center of Research (NCCR) Nano, Deutsche Forschungsgemeinschaft (DFG), Max-Planck-Society (MPG), Bundesministerium für Bildung und Forschung (BMBF), Japan Society for Promotion of Science (JSPS) and the ETH Zürich is greatly acknowledged.

## References

1 Bustamante, C. *et al.* (2004) Mechanical processes in biochemistry. *Annu. Rev. Biochem.* 73, 705–748
2 Hinterdorfer, P. and Dufrene, Y.F. (2006) Detection and localization of single molecular recognition events using atomic force microscopy. *Nat. Methods* 3, 347–355
3 Evans, E.A. and Calderwood, D.A. (2007) Forces and bond dynamics in cell adhesion. *Science* 316, 1148–1153
4 Kedrov, A. *et al.* (2007) Deciphering molecular interactions of native membrane proteins by single-molecule force spectroscopy. *Annu. Rev. Biophys. Biomol. Struct.* 36, 233–260
5 Borgia, A. *et al.* (2008) Single-molecule studies of protein folding. *Annu. Rev. Biochem.* 77, 101–125
6 Gerber, C. and Lang, H.P. (2007) How the doors to the nanoworld were opened. *Nat. Nanotechnol.* 1, 3–5
7 Neuman, K.C. and Nagy, A. (2008) Single-molecule force spectroscopy: optical tweezers, magnetic tweezers and atomic force microscopy. *Nat. Methods* 5, 491–505

8 Muller, D.J. and Dufrene, Y.F. (2008) Atomic force microscopy as a multifunctional molecular toolbox in nanobiotechnology. *Nat. Nanotechnol.* 3, 261–269
9 Moffitt, J.R. *et al.* (2008) Recent advances in optical tweezers. *Annu. Rev. Biochem.* 77, 205–228
10 Muller, D.J. *et al.* (2009) Force probing surfaces of living cells to molecular resolution. *Nat. Chem. Biol.* 5, 383–390
11 Dufrene, Y.F. *et al.* (2011) Five challenges to bringing single-molecule force spectroscopy into living cells. *Nat. Methods* 8, 123–127
12 Helenius, J. *et al.* (2008) Single-cell force spectroscopy. *J. Cell Sci.* 121, 1785–1791
13 Sheetz, M.P. (2001) Cell control by membrane-cytoskeleton adhesion. *Nat. Rev. Mol. Cell Biol.* 2, 392–396
14 Vogel, V. and Sheetz, M.P. (2009) Cell fate regulation by coupling mechanical cycles to biochemical signaling pathways. *Curr. Opin. Cell Biol.* 21, 38–46
15 Fletcher, D.A. and Mullins, R.D. (2010) Cell mechanics and the cytoskeleton. *Nature* 463, 485–492
16 Israelachvili, J. (1991) *Intermolecular and Surface Forces*, Academic Press Limited
17 Kedrov, A. *et al.* (2005) Locating ligand binding and activation of a single antiporter. *EMBO Rep.* 6, 668–674
18 Harris, A. (1973) Location of cellular adhesions to solid substrata. *Dev. Biol.* 35, 97–114
19 Cramer, L.P. and Mitchison, T.J. (1997) Investigation of the mechanism of retraction of the cell margin and rearward flow of nodules during mitotic cell rounding. *Mol. Biol. Cell* 8, 109–119
20 Eggert, U.S. *et al.* (2006) Animal cytokinesis: from parts list to mechanisms. *Annu. Rev. Biochem.* 75, 543–566
21 Barr, F.A. and Gruneberg, U. (2007) Cytokinesis: placing and making the final cut. *Cell* 131, 847–860
22 Straight, A.F. *et al.* (2003) Dissecting temporal and spatial control of cytokinesis with a myosin II Inhibitor. *Science* 299, 1743–1747
23 Miller, A.L. and Bement, W.M. (2009) Regulation of cytokinesis by Rho GTPase flux. *Nat. Cell Biol.* 11, 71–77
24 Carvalho, A. *et al.* (2009) Structural memory in the contractile ring makes the duration of cytokinesis independent of cell size. *Cell* 137, 926–937
25 Pollard, T.D. (2010) Mechanics of cytokinesis in eukaryotes. *Curr. Opin. Cell Biol.* 22, 50–56
26 Yang, L. *et al.* (2008) Modeling cellular deformations using the level set formalism. *BMC Syst. Biol.* 2, 68
27 Rappaport, T. (1996) *Cytokinesis in Animal Cells*, Cambridge University Press
28 Matzke, R. *et al.* (2001) Direct, high-resolution measurement of furrow stiffening during division of adherent cells. *Nat. Cell Biol.* 3, 607–610
29 Gibson, M.C. *et al.* (2006) The emergence of geometric order in proliferating metazoan epithelia. *Nature* 442, 1038–1041
30 Thery, M. and Bornens, M. (2006) Cell shape and cell division. *Curr. Opin. Cell Biol.* 18, 648–657
31 Kunda, P. and Baum, B. (2009) The actin cytoskeleton in spindle assembly and positioning. *Trends Cell Biol.* 19, 174–179
32 Maddox, A.S. and Burridge, K. (2003) RhoA is required for cortical retraction and rigidity during mitotic cell rounding. *J. Cell Biol.* 160, 255–265
33 Carreno, S. *et al.* (2008) Moesin and its activating kinase Slik are required for cortical stability and microtubule organization in mitotic cells. *J. Cell Biol.* 180, 739–746
34 Kunda, P. *et al.* (2008) Moesin controls cortical rigidity, cell rounding, and spindle morphogenesis during mitosis. *Curr. Biol.* 18, 91–101
35 McConnell, C.H. (1930) The mitosis found in hydra. *Science* 72, 170
36 Lechler, T. and Fuchs, E. (2005) Asymmetric cell divisions promote stratification and differentiation of mammalian skin. *Nature* 437, 275–280
37 Stewart, M.P. *et al.* (2011) Hydrostatic pressure and the actomyosin cortex drive mitotic cell rounding. *Nature* 469, 226–230
38 Krendel, M. *et al.* (2002) Nucleotide exchange factor GEF-H1 mediates cross-talk between microtubules and the actin cytoskeleton. *Nat. Cell Biol.* 4, 294–301
39 Mitchison, T.J. *et al.* (2008) Implications of a poroelastic cytoplasm for the dynamics of animal cell shape. *Semin. Cell Dev. Biol.* 19, 215–223
40 Blaser, H. *et al.* (2006) Migration of zebrafish primordial germ cells: a role for myosin contraction and cytoplasmic flow. *Dev. Cell* 11, 613–627
41 Paluch, E. and Heisenberg, C.P. (2009) Biology and physics of cell shape changes in development. *Curr. Biol.* 19, R790–R799
42 Bereiter-Hahn, J. (2005) Mechanics of crawling cells. *Med. Eng. Phys.* 27, 743–753
43 Fackler, O.T. and Grosse, R. (2008) Cell motility through plasma membrane blebbing. *J. Cell Biol.* 181, 879–884
44 Keren, K. *et al.* (2009) Intracellular fluid flow in rapidly moving cells. *Nat. Cell Biol.* 11, 1219–1224
45 Dietz, H. and Rief, M. (2006) Protein structure by mechanical triangulation. *Proc. Natl. Acad. Sci. U.S.A.* 103, 1244–1247
46 Kedrov, A. *et al.* (2006) Differentiating ligand and inhibitor interactions of a single antiporter. *J. Mol. Biol.* 362, 925–932
47 Kedrov, A. *et al.* (2008) Examining the dynamic energy landscape of an antiporter upon inhibitor binding. *J. Mol. Biol.* 375, 1258–1266
48 Kedrov, A. *et al.* (2010) Probing the interactions of carboxyatractyloside and atractyloside with the yeast mitochondrial ADP/ATP carrier. *Structure* 18, 39–46
49 Cisneros, D.A. *et al.* (2008) Transducer binding establishes localized interactions to tune sensory rhodopsin II. *Structure* 16, 1206–1213
50 Bippes, C.A. *et al.* (2009) Substrate binding tunes conformational flexibility and kinetic stability of an amino acid antiporter. *J. Biol. Chem.* 284, 18651–18663
51 Putney, L.K. and Barber, D.L. (2003) Na-H exchange-dependent increase in intracellular pH times G2/M entry and transition. *J. Biol. Chem.* 278, 44645–44649
52 Johnson, J.D. and Epel, D. (1976) Intracellular pH and activation of sea urchin eggs after fertilisation. *Nature* 262, 661–664
53 Lang, F. (ed.) (2006) *Mechanisms and Significance of Cell Volume Regulation*, Karger
54 Alexander, R.T. and Grinstein, S. (2006) Na+/H+ exchangers and the regulation of volume. *Acta Physiol. (Oxf.)* 187, 159–167
55 Wehner, F. *et al.* (2003) Cell volume regulation: osmolytes, osmolyte transport, and signal transduction. *Rev. Physiol. Biochem. Pharmacol.* 148, 1–80
56 Padan, E. *et al.* (2001) Na(+)/H(+) antiporters. *Biochim. Biophys. Acta* 1505, 144–157
57 Hunte, C. *et al.* (2005) Structure of a Na+/H+ antiporter and insights into mechanism of action and regulation by pH. *Nature* 435, 1197–1202
58 Muller, D.J. and Engel, A. (2007) Atomic force microscopy and spectroscopy of native membrane proteins. *Nat. Protoc.* 2, 2191–2197
59 Alsteens, D. *et al.* (2010) Force-induced formation and propagation of adhesion nanodomains in living fungal cells. *Proc. Natl. Acad. Sci. U.S.A.* 107, 20744–20749
60 Krieg, M. *et al.* (2008) Tensile forces govern germ-layer organization in zebrafish. *Nat. Cell Biol.* 10, 429–436
61 Lam, W.A. *et al.* (2011) Mechanics and contraction dynamics of single platelets and implications for clot stiffening. *Nat. Mater.* 10, 61–66
62 Cuerrier, C.M. *et al.* (2009) Real-time monitoring of angiotensin II-induced contractile response and cytoskeleton remodeling in individual cells by atomic force microscopy. *Pflugers Arch.* 457, 1361–1372
63 Kusche-Vihrog, K. *et al.* (2011) C-reactive protein makes human endothelium stiff and tight. *Hypertension* 57, 231–237
64 Roduit, C. *et al.* (2008) Elastic membrane heterogeneity of living cells revealed by stiff nanoscale membrane domains. *Biophys. J.* 94, 1521–1532
65 Rosenbluth, M.J. *et al.* (2008) Slow stress propagation in adherent cells. *Biophys. J.* 95, 6052–6059
66 Iyer, S. *et al.* (2009) Atomic force microscopy detects differences in the surface brush of normal and cancerous cells. *Nat. Nanotechnol.* 4, 389–393
67 Arboleda-Estudillo, Y. *et al.* (2010) Movement directionality in collective migration of germ layer progenitors. *Curr. Biol.* 20, 161–169
68 Strilic, B. *et al.* (2010) Electrostatic cell-surface repulsion initiates lumen formation in developing blood vessels. *Curr. Biol.* 20, 2003–2009
69 Prass, M. *et al.* (2006) Direct measurement of the lamellipodial protrusive force in a migrating cell. *J. Cell Biol.* 174, 767–772
70 Chaudhuri, O. *et al.* (2007) Reversible stress softening of actin networks. *Nature* 445, 295–298
71 Schillers, H. *et al.* (2010) Real-time monitoring of cell elasticity reveals oscillating myosin activity. *Biophys. J.* 99, 3639–3646